Parasitology Research (2019) 118:3223–3235
https://doi.org/10.1007/s00436-019-06461-0

ARTHROPODS AND MEDICAL ENTOMOLOGY - ORIGINAL PAPER

De novo transcriptome sequencing and differential gene expression analysis of two parasitic human *Demodex* species

Li Hu[1] · Yae Zhao[1] · Dongling Niu[1] · Xiaojuan Gong[1] · Rui Yang[1]

Received: 6 April 2019 / Accepted: 11 September 2019 / Published online: 6 November 2019

Abstract

Demodex are among the tiniest organisms in Acari and are important mammalian parasites. However, differences in pathogenicity between two human parasites, *Demodex folliculorum* and *Demodex brevis*, remain unknown. Related genetic studies are limited by RNA extraction difficulties and molecular data deficiencies. In this study, RNA extraction, de novo sequencing, functional annotation, and differential gene expression analyses were performed to compare *D. folliculorum* and *D. brevis*. This yielded 67.09 and 65.10 million clean reads, respectively, with similar annotations. Bioinformatics analyses and manual alignments identified 237 coding sequences comprising 48 genes from 29 families, including five important functional classes. Of these, 30 genes from 20 families related to metabolism, motion, detoxification and stress response, and allergic reaction were differentially expressed between the two species. Cathepsin type 1, serine protease inhibitor, arginine kinase, triosephosphate isomerase, muscle-specific protein 20-2, myosin alkaline light chain, troponin C, tropomyosin, and heat shock protein 90 were highly expressed in *D. folliculorum*, whereas cathepsin type 2, aspartic protease, serine protease, myosin heavy chain type 2, and alpha tubulin type 1C were highly expressed in *D. brevis*. Verified coding sequences were nearly consistent with unigene clusters. Further, absolute quantification results demonstrated that differentially expressed genes followed the predicted expression trend. Therefore, the first RNA sequencing and functional annotation analysis of two *Demodex* species was successful. Differential expression of important functional genes is likely implicated in pathogenicity disparities between these two species. Our study provides molecular data and technical support for further studies on human *Demodex* pathogenicity and functional genes.

Keywords Human *Demodex* · Pathogenicity differences · de novo transcriptome sequencing · Differentially expressed gene screening · Expression quantity verification

Introduction

Demodex comprises the tiniest mites among the Acari (Arthropods). Adults are slender, roughly 0.15–0.4 mm long and 0.05–0.06 mm wide. Further, they are globally distributed and parasitize the hair follicles, sebaceous glands, meibomian glands, and ceruminous glands of 11 mammalian orders including cattle, sheep, horses, pigs, dogs, cats, mice, and humans (Ayres 1930; Forton 2012; Olinda et al. 2013; Ferrer et al. 2014; Cornall and Wall 2015; Kabululu et al. 2015). *Demodex folliculorum* and *Demodex brevis* are two human parasite species that dwell in hair follicles and sebaceous glands, respectively. It was recently reported that in humans, this genus consists of pathogens that cause rosacea, blepharitis, acne, seborrheic dermatitis, and other common facial dermatoses (Zhao et al. 2010, 2011a, b, 2012a, b; Cheng et al. 2019; Gazi et al. 2019; Zeytun and Yazici 2019). Demodicidosis, an emerging dermatosis caused by mites (Zhao 2016), seriously endangers physical and mental health. However, differences in pathogenicity between *D. folliculorum* and *D. brevis* are unknown and represent a key component of demodicidosis-related research.

With the rapid development of molecular biological technology, a growing number of studies have shown that functional gene research is an effective way to elucidate

Section Editor: Xing-Quan Zhu

Electronic supplementary material The online version of this article (https://doi.org/10.1007/s00436-019-06461-0) contains supplementary material, which is available to authorized users.

✉ Yae Zhao
zhaoyae@xjtu.edu.cn; zhaoyae@sina.com

[1] Department of Pathogen Biology and Immunology, School of Basic Medical Sciences, Xi'an Jiaotong University, No.76 Yanta West Road, Xi'an 710061, China

pathogenic mechanisms (Conte et al. 2011; Liu et al. 2011). However, *Demodex* studies at the RNA level have been challenging for four reasons. First, *Demodex* are microscopic, and *D. brevis* is especially small. Second, few individuals are moderately or severely infected by *Demodex*, and mites are difficult to preserve in vitro as they autolyze after 1 or 2 days (Zhao et al. 2009, 2011c). Third, *Demodex* are host species-specific and cannot be cultured in vitro, and thus, standardized mites are not available for experimentation. Last, the chitinous exoskeleton of mites directly reduces the quality of extracted RNA, which often fails to meet the requirements for molecular biology experiments. To date, neither functional gene nor transcriptome data for *Demodex* are available from GenBank or the SRA (Sequence Read Archive).

Genome-wide Demodicidae data have not been previously reported, and thus, there are no reference genomes for *Demodex* transcriptome assembly. De novo sequencing can be performed based on the functional genes of closely related species. However, transcriptome data for Cheyletidae, to which *Demodex* belongs, is currently unavailable from GenBank. Therefore, the transcriptome data of relatively genetically dissimilar mites must be used, including those of agricultural mites of Tetranychidae (Grbić et al. 2011), Varroidae (Conte et al. 2011), and Phytoseiidae (Hoy et al. 2013), as well as the medically important mites of Dermanyssidae (Schicht et al. 2013), Acaridae (Stuglik et al. 2014), Pyroglyphidae (Chan et al. 2015), and Psoroptidae (He et al. 2016). These annotations have laid the foundation for the RNA sequencing (RNA-Seq) and annotation of *Demodex*.

To explore the pathogenic mechanisms of two parasitic human *Demodex* species at the gene level, this study was performed to obtain novel de novo transcriptome sequencing and functional annotation data for *D. folliculorum* and *D. brevis* using a high-throughput sequencing platform. Differentially expressed homologous genes of the two *Demodex* species were screened and specific primers were designed to detect nucleotide sequences. Further, a prokaryotic expression system was constructed for proteins and an absolute real-time quantitative PCR (RT-qPCR) method was established to verify expression levels. Therefore, this study offers a novel analysis of *Demodex* at the RNA level, providing molecular data and technical support for the study of functional genes and pathogenicity differences for two parasitic human *Demodex* species, namely *D. folliculorum* and *D. brevis*.

Materials and methods

Mite collection and RNA extraction

Living *D. folliculorum* and *D. brevis* adults were collected from the faces of six human subjects with oily skin in Xi'an, China, using transparent adhesive tape. *Demodex* mites were identified under a microscope (Motic 2.0, Motic, Xiamen, China) according to their shape, body size, opisthosoma content, and especially, the shape of the opisthosoma terminus (Zhao et al. 2013). Three subjects harbored *D. folliculorum* and three subjects harbored *D. brevis.* The two *Demodex* mite species were quickly collected using a customized needle that was comprised of a syringe, a pipette tip, and a pin. RNA was extracted according to the methods of Zhao et al. (2016) with slight modifications, then sent to Wuhan BGI Clinical Laboratory Co. for quality assessment using an Agilent 2100 Bioanalyzer System (Agilent Technologies, Palo Alto, CA, USA). RNA samples with quantity ≥ 10 ng and an RNA integrity number (RIN) ≥ 5.0 met the minimum requirements specified by Wuhan BGI Clinical Laboratory for cDNA library construction and RNA-Seq. Eventually, RNA samples extracted from 191 *D. folliculorum* mites and 326 *D. brevis* mites were used.

cDNA library construction and de novo RNA-Seq

Respective mRNA-seq libraries were prepared for *D. folliculorum* and *D. brevis* according to the Illumina® TruSeq® RNA sample preparation protocol (Illumina Inc., San Diego, CA, USA). After digesting residual genomic DNA in the total RNA by DNase I, mRNA was accumulated using oligo (dT)-attached magnetic beads, then fragmented, and reverse-transcribed into first-strand cDNA (ss cDNA). Then, the second strand of cDNA (ds cDNA) was synthesized, and the sticky-end was repaired and ligated with an "A" base and adaptor at the 3′ end. Finally, ds cDNA of an appropriate size was purified for PCR amplification to create the cDNA library. The qualified libraries of the two *Demodex* species, determined using an Agilent 2100 Bioanalyzer System (Agilent Technologies) and an ABI StepOnePlus™ Real-Time PCR System (Applied Biosystems, Foster City, CA, USA), were respectively sequenced on the Illumina HiSeq 4000 sequencing platform (Illumina Inc.) to obtain raw reads.

De novo assembly and functional annotation

Clean reads were obtained by filtering low quality reads. The proportions of Q20 and Q30 clean reads were calculated. De novo transcripts were assembled using Trinity software (v.2.0.6, parameters: –min_contig_length150 –CPU 8–min_kmer_cov 3–min_glue3–bfly_opts '-V 5–edge-thr=0.1–stderr'), then clustered by Tgicl (version: v.2.0.6, parameters: -l 40 -c 10 -v 25 -O '-repeat_stringency 0.95 -minmatch 35 -minscore 35') to remove unigene redundancy. Unigenes were annotated by alignment with the non-redundant proteins (NR), non-redundant nucleotide (NT), clusters of orthologous groups (COG), Kyoto Encyclopedia of Genes and Genomes (KEGG), Swiss Protein (SwissProt), Gene Ontology (GO),

and InterPro databases. NT, NR, COG, KEGG, and SwissProt annotations were conducted by Blast (http://blast.ncbi.nlm.nih.gov/Blast.cgi, v.2.2.23 with default parameters). GO annotation was completed based on NR annotation using Blast2GO (https://www.blast2go.com, v.2.5.0 with default parameters). InterPro annotation was conducted by InterProScan5 (https://code.google.com/p/interproscan/wiki/Introduction, v.5.11-51.0 with default parameters). The CDSs of annotated unigenes were predicted in the following priority order: NR, SwissProt, KEGG, and COG; those of unannotated unigenes were predicted by ESTScan (http://sourceforge.net/projects/estscan, v.3.0.2 with default parameters).

Calculation of unigene expression quantities

Clean reads were mapped to unigenes using the Bowtie 2 tool (http://bowtie-bio.sourceforge.net/ Bowtie2 /index.shtml, v.2.2.5, parameter: -q –phred64 –sensitive –dpad 0 –gbar 99999999 –mp 1,1 –np 1 –score-min L,0,-0.1 -I 1 -X 1000 –no-mixed –no-discordant -p 1 -k 200). The FPKM method was used to calculate unigene expression quantities. A distribution histogram was plotted with the expression quantity on the x-axis and the proportion of unigenes on the y-axis. The number of unigenes that had an expression quantity ≥ 100 and were assigned to species closely related to *Demodex* in Acari were compared between *D. folliculorum* and *D. brevis*.

Important functional gene screening and analysis of DEGs

Five classes of important *D. folliculorum* and *D. brevis* functional genes ("metabolic enzyme," "allergen," "motion-related," "detoxification and stress response-related," and "mitochondrial") were screened from NR and NT annotation results. The CDSs of these genes were confirmed by bioinformatics methods combined with manual alignments. First, unigene open reading frames were predicted using the ORF Finder program (https://www.ncbi.nlm.nih.gov/orfnder/) and then aligned by BLAST (https://blast.ncbi.nlm.nih.gov/Blast.cgi) to predict gene function. Then, unigenes of the two *Demodex* species that matched the same gene were further analyzed by DNAssist v.2.2, Clustal X v.1.8, and MEGA v.5.0 for homology comparisons. Finally, using the CDSs of closely related species as templates, the length and expression quantity of *D. folliculorum* and *D. brevis* CDSs were confirmed. The fold change (FC) in gene expression between *D. folliculorum* and *D. brevis* and the corresponding log2FC values were calculated to compare differences. Differentially expressed genes (DEGs) were identified as genes with a log2FC ≥ 1 or log2FC ≤ −1, where log2FC ≥ 1 represented higher expression in *D. folliculorum* and log2FC ≤ −1 represented higher expression in *D. brevis*.

CDS verification of homologous genes

RNA was reverse transcribed to ss cDNA and then synthesized into ds cDNA according to the methods of Hu et al. (2015). Homologous genes of the two *Demodex* species were verified using specific primers (Supplementary Table S1) with PrimeSTAR® HS DNA Polymerase (TaKaRa, Tokyo, Japan). PCR products were detected by 1.5% TAE agarose gel electrophoresis, purified using a Gel Extraction Kit (OMEGA Bio-Tek, Norcross, GA, USA), cloned with a pMD19-T vector (TaKaRa), and sequenced by GENEWIZ Co. Ltd. (Suzhou, China). The CDSs obtained in this study and those predicted from unigenes were aligned under a multiple alignment model in Clustal X v.1.8, and then MEGA v.5.0 was used to calculate the sequence identities of the adjusted nucleotides and amino acids. The obtained sequences were submitted to GenBank.

Prokaryotic expression verification

The amino acid composition, protein molecular weight, and isoelectric point of the triosephosphate isomerase (*TPI*) gene were predicted by ProtParam (https://web.expasy.org/protparam/). Primers with Ecor I and Xho I restriction sites were then designed to construct a pET32a-*TPI* expression vector. PET32a (+)-*TPI* was then transformed into *Escherichia coli* BL21 (Tiangen, Beijing, China) and induced to express TPI protein using 0.4 mM/L isopropyl β-D-1-thiogalactopyranoside (Sigma-Aldrich, St. Louis, MO, USA). TPI was isolated after bacteria were cultured for 0, 1, 2, 3, 4, 5, and 6 h by sodium dodecyl sulfate polyacrylamide gel electrophoresis (SDS-PAGE). The recombinant TPI protein was observed by Coomassie® Brilliant Blue R250 (Amresco, Solon, OH, USA) staining. Next, the recombinant TPI protein was transferred onto a polyvinylidene di-fluoride (PVDF) membrane (Millipore, Billerica, MA, USA). After incubation in a blocking solution of 5% skimmed milk in Tris-buffered saline containing 0.1% Tween-20 for 1 h at room temperature, the membrane was probed using an anti-His-tag mouse monoclonal antibody diluted 1:2000 (v/v) (Abclonal, Boston, MA, USA) overnight at 4 °C, followed by incubation with horseradish peroxidase-labeled goat anti-mouse IgG (HRP-IgG) diluted 1:2000 (v/v) (Neobioscience, Shenzhen, China) for 1 h at room temperature. Western blot analysis was conducted to analyze protein specificity. Immunoreactive proteins were visualized by incubation in ECL solution (Millipore, Billerica, MA, USA). Images were captured using a Fusion FX5 camera system.

Expression quantity verification

Primers for RT-qPCR were designed (Supplementary Table S2) and verified by conventional PCR, cloning, and

sequencing. Plasmid DNA was extracted using a Plasmid Mini Kit (OMEGA Bio-Tek, Norcross, GA, USA), and the concentration (g/μL) was measured by an ultraviolet spectrophotometer (Thermo Fisher Scientific Inc., Waltham, MA, USA). The DNA copy number/μL of plasmid was calculated as $6.02 \times 10^{23} \times$ plasmid concentration / ((vector 2692 bp + objective fragment length) × 660 Da/bp). Six plasmid gradients ranging from 10^2 to 10^7 copies/μL were diluted to produce a standard curve. The *D. folliculorum* and *D. brevis* RNA remaining after RNA-Seq was reverse transcribed to ss cDNA in a final volume of 20 μL using M-MLV reverse transcriptase (TaKaRa). One microliter of ss cDNA was used as a template for each reaction containing 1 μL ss cDNA, 10 μL SYBR Premix Ex Taq (TaKaRa), 8 μL ddH2O, and 0.5 μL of each primer (10 μM). Three replicates were conducted for each sample. The absolute copy number per ng ss cDNA was calculated according to the cycle threshold value and standard curve, and the fold change of each gene between the two *Demodex* species was calculated.

Results

RNA quality

Agilent 2100 detection results showed that the quality of RNA from 191 *D. folliculorum* mites and 326 *D. brevis* mites was grade D, as the quantity and concentration of RNA were lower than 0.2 μg and 20.0 ng/μL, respectively, and the baseline was slightly elevated and not smooth enough (Fig. 1; Hu et al. 2016). However, the RIN values were 6.5 and 5.6, and the quantities were 10.2 ng and 10.8 ng, respectively. These values basically met the requirements for cDNA library construction and RNA-Seq using a tiny amount of RNA as proposed by Wuhan BGI Clinical Laboratory Co. (Wuhan, China).

Quality of RNA sequencing data

For *D. folliculorum*, 67.78 million raw reads were obtained, of which 98.98% were clean reads (67.09 Mb). Clean read values for Q20 and Q30 were 95.78% and 90.56%, respectively. A total of 49,573 unigenes were assembled, of which 51.57% were longer than 1000 bp. For *D. brevis*, 65.6 Mb raw reads were obtained, of which 99.24% were clean reads (65.10 Mb). Clean read values for Q20 and Q30 were 94.94% and 89.23%, respectively. A total of 67,363 unigenes were assembled, of which 51.04% were longer than 1000 bp (Table 1). These results indicated good quality sequencing and assembly data for the two *Demodex* species. The raw sequence data sets are available in the SRA database (accession numbers: SRR8351662 and SRR8351661).

Functional annotation

For *D. folliculorum*, 32,303 of the 49,573 unigenes (65.16%) were annotated based on seven functional databases (Table 2), of which 13,442 were simultaneously annotated using NR, COG, KEGG, SwissProt, and Interpro databases. For *D. brevis*, 52,144 of 67,363 unigenes (77.41%) were annotated, of which 15,791 were simultaneously annotated by the same five databases. A total of 28,633 and 37,774 CDSs were detected for *D. folliculorum* and *D. brevis*, respectively.

NR annotation results

A total of 27,429 and 35,720 unigenes were annotated to *D. folliculorum* and *D. brevis*, respectively. The most frequently annotated species were *Stegodyphus mimosarum*, *Ixodes scapularis*, *Metaseiulus occidentalis*, and *Zootermopsis nevadensis* (Fig. 2). It was worth noting that mites accounted for only 6.46% and 6.56% of the *D. folliculorum* and *D. brevis* unigenes, respectively. *M. occidentalis* of Phytoseiidae accounted for 5.66% of both *D. folliculorum* and *D. brevis* unigenes, whereas other mites accounted for even less in the following order: Tetranychidae (*D. folliculorum*, 0.68%, and *D. brevis*, 0.72%), Oribatei (*D. folliculorum*, 0.05%, and *D. brevis*, 0.06%), Acaridae (*D. folliculorum*, 0.02%, and *D. brevis*, 0.04%), Sarcoptidae (*D. folliculorum*, 0.02%, and *D. brevis*, 0.01%), Pyrgomorphidae (*D. folliculorum*, 0.01%, and *D. brevis*, 0.03%), and Psoroptidae (*D. folliculorum*, 0.01%, and *D. brevis*, 0.01%) (Supplementary Table S3). Regrettably, Cheyletidae, to which *Demodex* belongs, did not account for any of the unigenes, owing to the lag in Cheyletidae research and the lack of molecular data in GenBank.

GO annotation results

Based on sequence identities, 5712 *D. folliculorum* unigenes were annotated to 23 groups of biological processes (BPs), 19 groups of cellular components (CCs), and 12 groups of molecular functions (MFs), whereas 8134 *D. brevis* unigenes were annotated to 24 groups of BPs, 17 groups of CCs, and 14 groups of MFs. A similar unigene category distribution was observed for the two *Demodex* species. For BPs, "cellular process," "metabolic process," and "single-organism process" were the three largest groups for both species, whereas the smallest groups were "rhythmic process" and "hormone secretion" for *D. folliculorum* and "biological regulation" and "hormone secretion" for *D. brevis*. For CCs, "cell," "cell part," and "membrane" were the largest groups for both species, whereas the smallest groups were "nucleoid," "virion," and "virion part" for *D. folliculorum* and "nucleoid," "extracellular matrix," and "collagen trimer" for *D. brevis*. For MFs, the largest groups were "catalytic activity" and "binding" for both

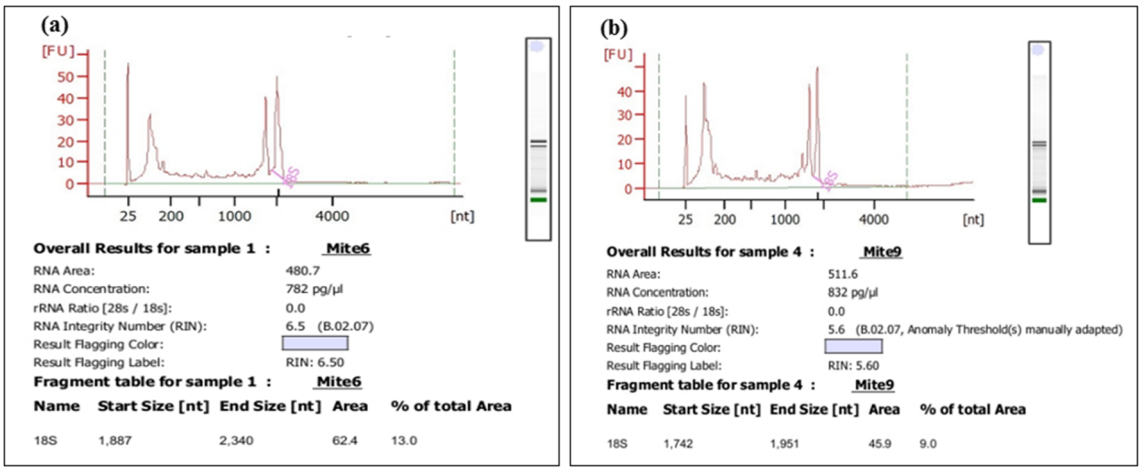

Fig. 1 RNA concentration and RNA integrity detected by Agilent 2100: **a** 191 *Demodex folliculorum* mites; **b** 326 *Demodex brevis* mites

species, whereas the smallest groups were "antioxidant activity" and "electron carrier activity" for *D. folliculorum* and "receptor regulator activity" and "channel regulator activity" for *D. brevis* (Fig. 3).

COG annotation results

As shown in Fig. 4, 15,102 *D. folliculorum* unigenes and 17,500 *D. brevis* unigenes were assigned to 25 functional COG categories with similar annotation results. For both species, the largest category was "general function prediction only," followed by "transcription" and "replication, recombination, and repair." The smallest categories were "nuclear structure" and "extracellular structure."

KEGG annotation results

A total of 24,636 *D. folliculorum* unigenes and 30,891 *D. brevis* unigenes were annotated to six groups of 42 pathways by KEGG (Fig. 5). For both species, the two largest pathways were "signal transduction" and "global map," and the most pathogenesis-related pathway appeared to be "infectious diseases: parasitic, viral, bacteria."

Table 1 Unigene quality detection of the two *Demodex* species

Index	Unigene	
	D. folliculorum	*D. brevis*
Total number	49,573	67,363
Total length (bp)	113,306,557	119,779,401
Mean length (bp)	2285	1778
N50 (bp)	4299	3344
N70 (bp)	2920	2188
N90 (bp)	1234	843
GC%	32.98	27.69

Gene expression analysis

Figure 6 shows the fragments per kilobase of exon model per million mapped reads (FPKM) unigene distribution. For *D. folliculorum*, 44,514 unigenes had FPKM values that ranged from 0.01 to 238,590 (median 1.66), of which 185 had FPKM values > 100 (0.42%). Of those 185 unigenes, unigenes assigned to species in Acari accounted for 29.19% (54/185). The six unigenes with FPKM values ≥ 1000 were assigned to ribosomal or mitochondrial *Demodex* genes. The six unigenes with FPKM values from 500 to 1000 were assigned to GTP-binding protein (886.42) and fructose 1,6-bisphosphate aldolase (578.44) of *I. scapularis*, tropomyosin (Tm) of *Dermatophagoides pteronyssinus* (566.61), actin of *Ornithodoros moubata* (553.66), and selenium dependent salivary glutathione peroxidase of *I. scapularis* (553.52). The other 42 unigenes had FPKM values that ranged from 100 to 500.

For *D. brevis*, 60,852 unigenes had FPKM values that ranged from 0.01 to 72,766 (median 2.97), of which 146 unigenes had FPKM values > 100 (0.24%). Of those 146 unigenes, unigenes assigned to Acari species accounted for 28.08% (41/146). The 10 unigenes with FPKM values ≥ 500 were assigned to *Demodex* ribosomal or mitochondrial genes. The other 31 unigenes had FPKM values that ranged from 100 to 500. The top five unigenes with higher FPKM values were assigned to AV422 of *Amblyomma americanum* (499.38), actin of *O. moubata* (478.76), glucose-6-phosphatase (473.8) and glyceraldehyde 3-phosphate dehydrogenase (396.63) of *I. scapularis*, and vitellogenin of *Panonychus citri* (395.12).

Screening of important functional genes

From the NR and NT annotation results, 16 metabolic enzyme-encoding genes, 23 *Dermatophagoides* allergen genes, 9 motion-related genes, 9 detoxification and

Table 2 Unigene annotation results from the seven functional databases of the two *Demodex* species

Database	*D.folliculorum*		*D.brevis*	
	Number of unigenes	Percentage (%)	Number of unigenes	Percentage (%)
NR	27,429	55.33	35,720	53.03
NT	20,202	40.75	39,943	59.30
SwissProt	25,714	51.87	32,738	48.60
COG	15,102	30.46	17,500	25.98
KEGG	24,636	49.70	30,891	45.86
GO	5712	11.52	8134	12.07
Interpro	23,998	48.41	30,338	45.04
Total	32,303/49,573	65.16	52,144/67,363	77.41

stress-response genes, and 7 mitochondrial genes were screened from the two *Demodex* species (Supplementary Table S4). Through bioinformatics analysis and manual alignment, 237 unigenes of 48 genes from 29 families were identified, all of which had FPKM values > 1.0 as follows: 122 unigenes of 19 genes from 12 families identified as encoding metabolic enzymes, of which 75 unigenes had complete CDSs; 82 unigenes of 15 genes from 10 families identified as encoding allergens, of which 63 unigenes had complete CDSs; 46 unigenes of 9 genes from 7 families identified as motion-related, of which 34 had complete CDSs; 67 unigenes of 13 genes from 3 families identified as detoxification and stress response-related, involving glutamate-gated chloride channels, gamma-aminobutyric acid receptors, and heat shock proteins. One unigene of both *D. folliculorum* and *D. brevis* was identified as a nearly complete mitochondrial gene involving the complete CDS of seven functional genes, namely *cox*1, *cox*2, *cox*3, *ATP*6, *ATP*8, *ND*3, and *ND*5 (Supplementary Table S5).

Analysis of DEGs

Among the 48 genes of 29 families in the five identified functional classes, 30 genes of 20 families from four classes (metabolic enzymes, motion-related, detoxification and stress response-related, and allergic reaction) were differentially expressed between the two *Demodex* species according to the criterion $|\log2FC \geq 1|$ (Table 3). Among metabolic enzyme-encoding genes, *D. folliculorum* harbored six highly expressed genes, which were mainly involved in energy metabolism, immune regulation, proteolysis, and protein folding. *D. brevis* showed seven highly expressed genes, which were mainly involved in peptide hydrolysis, synthesis and degradation of chitin, and antioxidation. Among the motion-related genes, *D. folliculorum* showed five significantly enriched genes with higher FPKM and fold change values (*D. folliculorum*, 1513.41 vs *D. brevis*, 36.04; *D. folliculorum*, 672.84 vs *D. brevis*, 23.91), which were involved in the occurrence and differentiation of muscle fibers, muscle movement and metabolism, and intracellular microtubule composition. Although *D. brevis* also showed two highly expressed genes, the FPKM and fold change values (*D. brevis*, 26.15 vs *D. folliculorum*, 3.46; *D. brevis*: 31.85 vs *D. folliculorum*: 2.07) were relatively lower. Among the detoxification and stress response genes, *D. folliculorum* showed seven highly expressed genes and *D. brevis* showed only three. It should be noted that 10 of the 30 DEGs matched *Dermatophagoides* allergens, of which 9 were more highly expressed in *D. folliculorum* than in *D. brevis*.

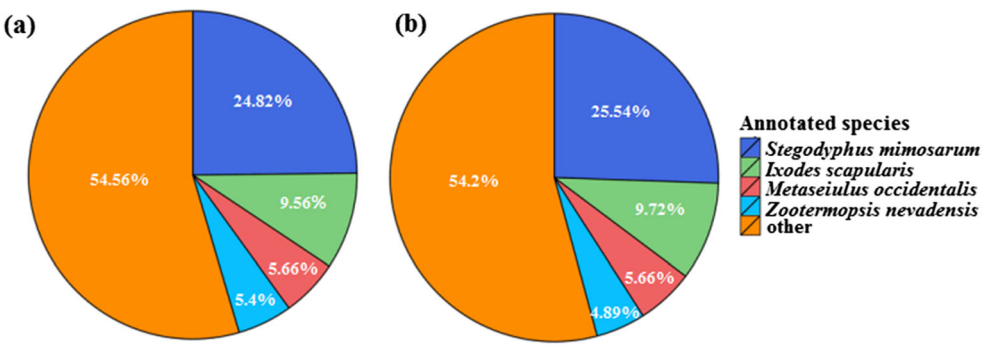

Fig. 2 Species distribution of unigenes annotated by NR: **a** 27,429 unigenes of *Demodex folliculorum*; **b** 35,720 unigenes of *Demodex brevis*

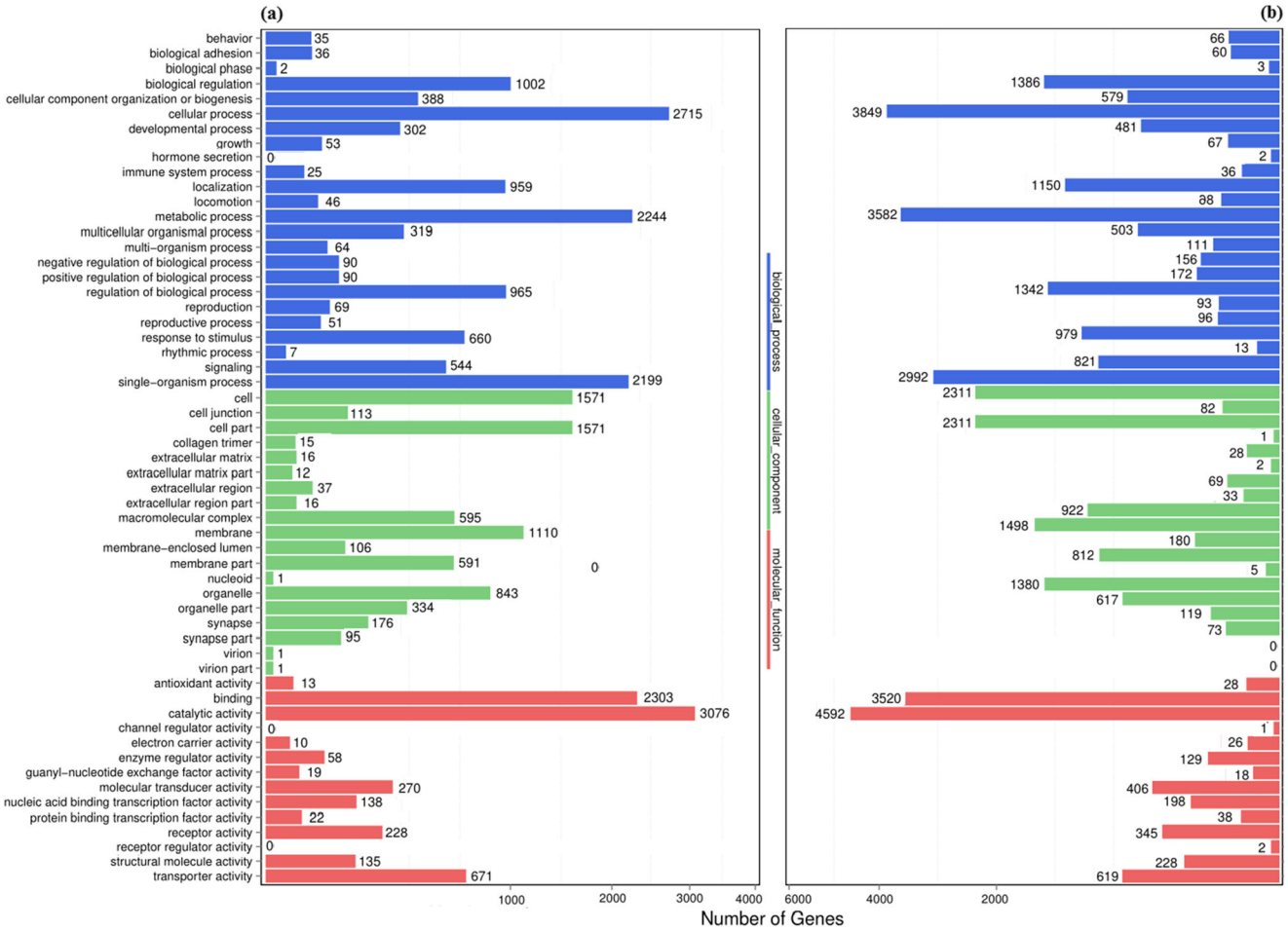

Fig. 3 Histogram presentation of GO classification of unigenes: **a** 5712 unigenes of *Demodex folliculorum*; **b** 8134 unigenes of *Demodex brevis*

CDS verification of homologous DEGs

Twenty-three of the 29 gene families were homologous between *D. folliculorum* and *D. brevis*. The verified CDSs (accession numbers: MK343724–MK343741, MK302784–MK302802) were completely or nearly identical to the unigenes, except for small differences in *D. brevis Tm*, myosin alkali light chain, and *TPI*. In *Tm*, there was an incorrect assembly of 185 bp at the 5′ terminus (Supplementary Fig. S1a) of the unigene. After adjustment, the unigene and the verified CDSs showed nucleotide identities of 99.06–100% and amino acid identities of 97.50–100% (Supplementary

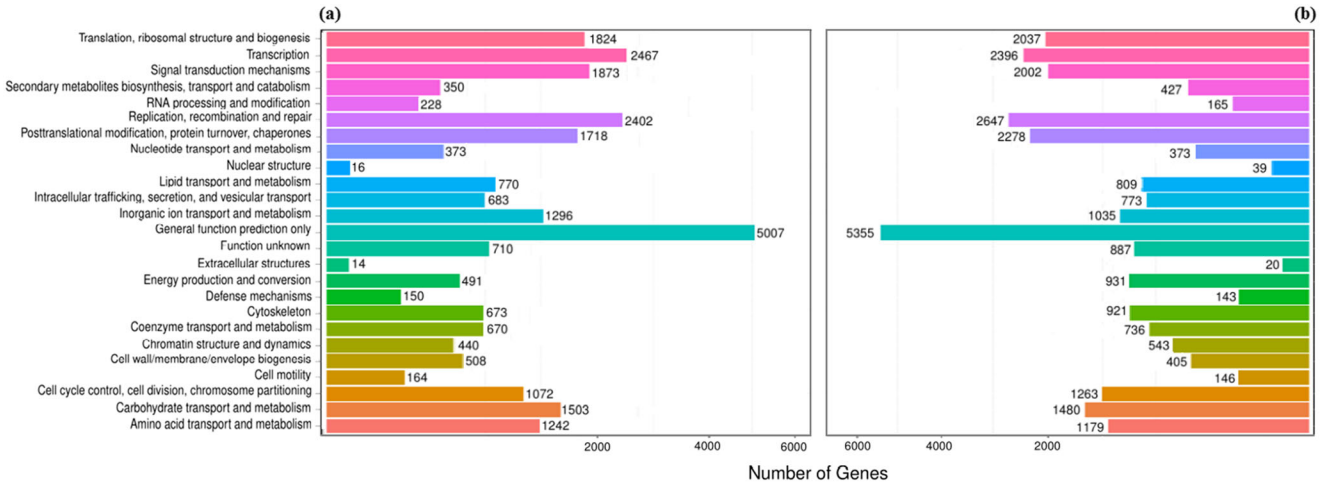

Fig. 4 COG annotation of putative proteins of the unigenes: **a** 15,102 unigenes of *Demodex folliculorum*; **b** 17,500 unigenes of *Demodex brevis*

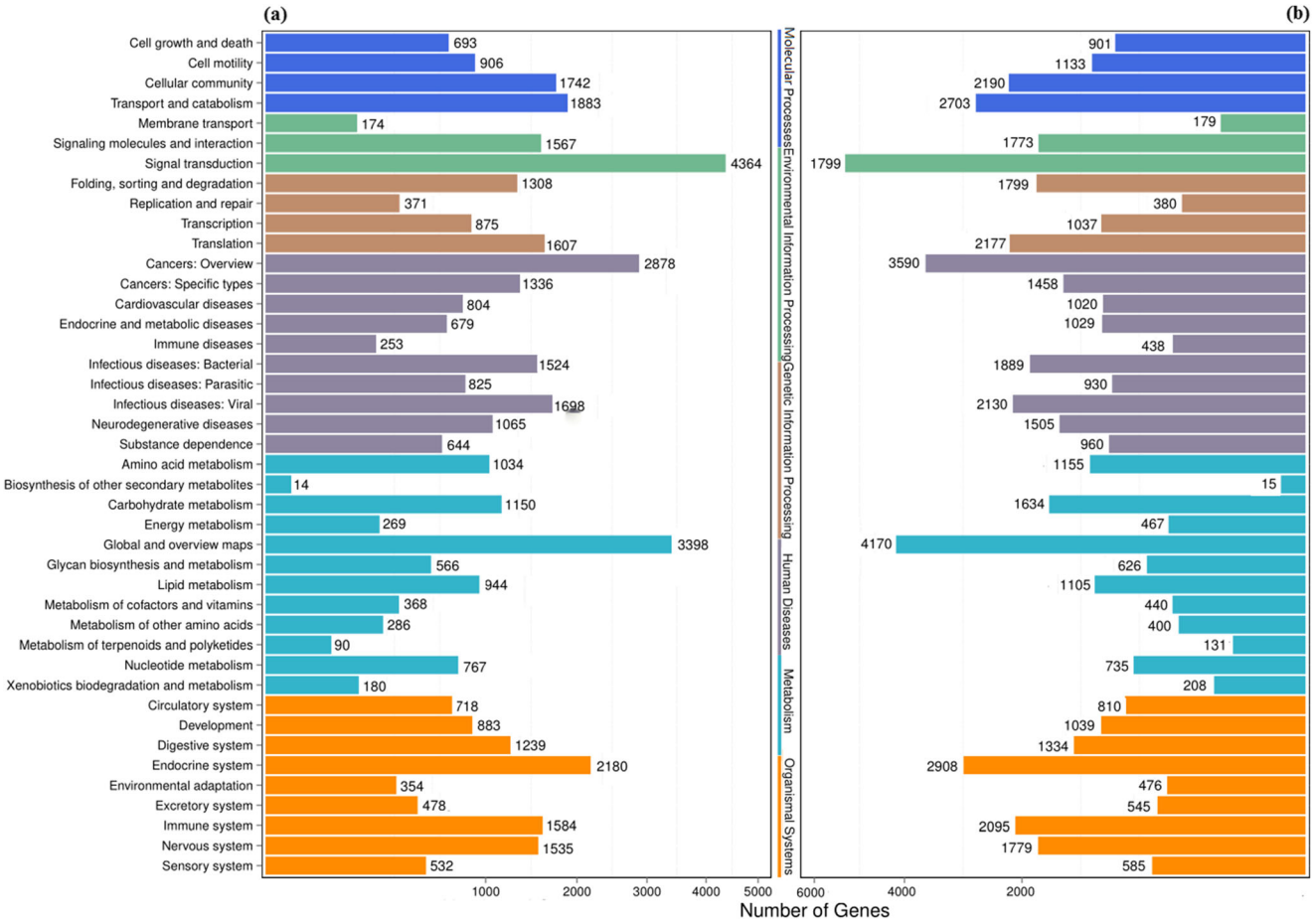

Fig. 5 Pathway assignment of unigenes based on KEGG: **a** 24,636 unigenes of *Demodex folliculorum*; **b** 30,891 unigenes of *Demodex brevis*

Fig. S1b). In the myosin alkali light chain unigenes, there was an insertion of 74 bp (Fig. S2a). After discounting this insertion, the unigenes and the verified CDSs showed nucleotide identities of 99.58–100% and amino acid identities of 98.74–100% (Supplementary Fig. S2b). In *TPI*, there were two exogenous unigene insertions of 67 bp and 79 bp (Supplementary Fig. S3a). After discounting these insertions, the unigenes and the verified CDSs showed 100% nucleotide identities and 100% amino acid identities (Supplementary Fig. S3b).

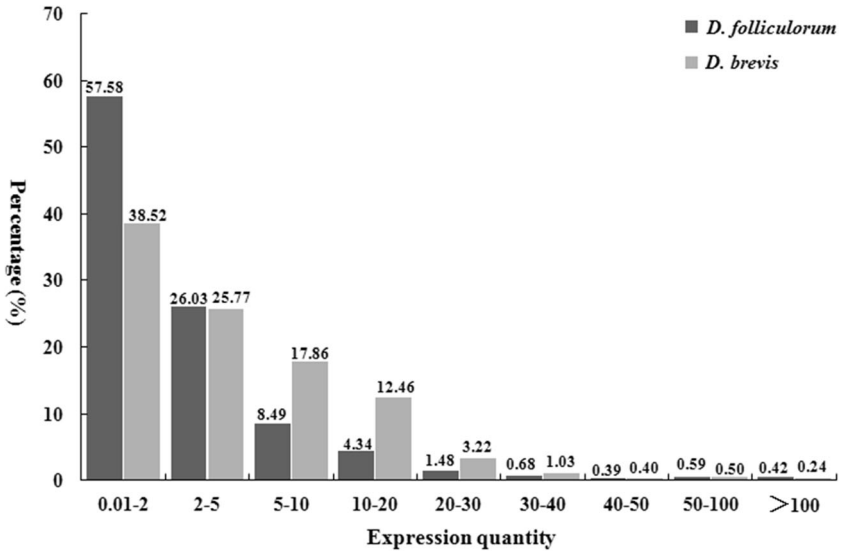

Fig. 6 Distribution of unigenes with different expression quantity of *Demodex folliculorum* and *Demodex brevis*

Table 3 Differently expressed genes between the two *Demodex* species

Function	Gene	*D. f*-CDS		*D. b*-CDS		FC (*D.f* vs *D.b*)	
		Len (bp)	FPKM	Len (bp)	FPKM	Ratio	Log2
Metabolic enzyme	*Cathepsin type 1*	*1071*	*110.56*	–	–	+∞	+∞
	Cysteine protease (Der f 1)	*1677*	*9.13*	–	–	+∞	+∞
	Serpin (Der f 27)	*1362*	*317.36*	*1356*	*22.03*	*14.41*	*3.85*
	Arginine kinase (Der f 20)	*1071*	*438.10*	*1071*	*58.24*	*7.52*	*2.91*
	Triosephosphate isomerase (Der f 25)	*744*	*109.61*	*823*	*26.04*	*4.21*	*2.07*
	Peptidyl-prolyl cis-trans isomerase like (Der f 29)	*552*	*12.72*	*755*	*5.16*	*2.47*	*1.30*
	Thioredoxin peroxidase 10-2	**570**	**3.21**	**480**	**7.94**	**0.40**	**−1.31**
	Cathepsin type 2	**990**	**45.79**	**1062**	**149.48**	**0.31**	**−1.71**
	Chitinase type 10 (Der f 15)	**1902**	**4.76**	**2028**	**15.58**	**0.31**	**−1.71**
	Chitin synthetase	**2987**	**3.07**	**2790**	**17.74**	**0.17**	**−2.53**
	Serine protease	**480**	**3.77**	**750**	**27.43**	**0.14**	**−2.86**
	Aspartic protease type 2	–	–	**1161**	**8.23**	−∞	−∞
	Aspartic protease type 1	–	–	**1173**	**74.12**	−∞	−∞
Motion related	*Muscle-specific protein type 20-2*	*561*	*1513.41*	*561*	*36.04*	*41.99*	*5.39*
	Myosin alkali light chain (Der f 26)	*483*	*672.84*	*483*	*23.91*	*28.14*	*4.81*
	Troponin C	*459*	*332.06*	*459*	*19.78*	*16.79*	*4.07*
	Tropomyosin (Der f 10)	*855*	*566.61*	*855*	*70.15*	*8.08*	*3.01*
	α-Tubulin type 1(Der f 33)	*1356*	*506.72*	*1356*	*154.37*	*3.28*	*1.71*
	Myosin heavy chain type 2	**2487**	**3.46**	**2046**	**26.15**	**0.13**	**−2.92**
	α-Tubulin type 1C	**646**	**2.07**	**654**	**31.85**	**0.06**	**−3.94**
Detoxification	*Glutamate gate chloride ion channel type 2*	*924*	*6.75*	/	/	+∞	+∞
	Glutamate gate chloride ion channel type 4	*940*	*31.51*	*1174*	*2.30*	*13.70*	*3.78*
	Glutamate gate chloride ion channel type 1	*1443*	*45.40*	*1167*	*20.99*	*2.16*	*1.11*
	γ-Aminobutyric acid receptor α subunit	*816*	*16.79*	–	–	+∞	+∞
	γ-Aminobutyric acid receptor B subunit type 1-like	*489*	*23.58*	*589*	*8.74*	*2.70*	*1.43*
	γ-Aminobutyric acid receptor B subunit type 2-like	**2229**	**5.41**	**1728**	**14.16**	**0.38**	**−1.39**
	Glutamate gate chloride ion channel type 5-1	**325**	**1.11**	**653**	**2.43**	**0.46**	**−1.13**
	Glutamate gate chloride ion channel type 5-2	–	–	**621**	**26.26**	−∞	−∞
Stress response	*Heat shock protein 90*	*2268*	*404.13*	*1386*	*33.08*	*12.22*	*3.61*
	Heat shock protein 70-3 (Der f 28)	*1992*	*133.74*	*2062*	*63.99*	*2.09*	*1.06*

Italic represents higher expression level in *D. f* than in *D. b*; bold represents higher expression level in *D. b* than in *D. f*

D. f: *Demodex folliculorum*, *D. b*. *Demodex brevis*, *Der f x* group x allergen from *Dermatophagoides farinae*, *Len* length, *FC* fold change

TPI verification by prokaryotic expression

To further verify the reliability of CDS data and provide a foundation for functional studies in the future, the *TPI* gene, which had been verified and adjusted during the CDS verification of homologous genes, was selected for prokaryotic expression. ProtParam analysis showed that the TPI protein was comprised of 247 amino acids with a predicted mass of approximately 27 kDa for the two *Demodex* species. The theoretical isoelectric point was 5.68 for *D. folliculorum* and 6.60 for *D. brevis*. SDS-PAGE showed that at different times of induction, a protein band near 43 kDa was obviously expressed, representing a weight similar to that of the pET32a (+) TPI fusion protein (44.9 kDa; his-tag, 17.9 kDa + TPI, 27 kDa), indicating that the recombinant protein was successfully expressed (Fig. 7 a and b). Western blot analysis demonstrated that the expressed protein near 43 kDa could be recognized by an anti-His (C-terminal) antibody (Fig. 7 c and d), suggesting that recombinant TPI was specifically expressed and that the adjusted *TPI* sequences were correct.

DEG verification by absolute quantification

Considering that *D. folliculorum* and *D. brevis* are two separate species, we used absolute RT-qPCR to verify the DEGs; for this, we used genes that had been reported in other mites, and those with an expression quantity value ≥ 20 in each

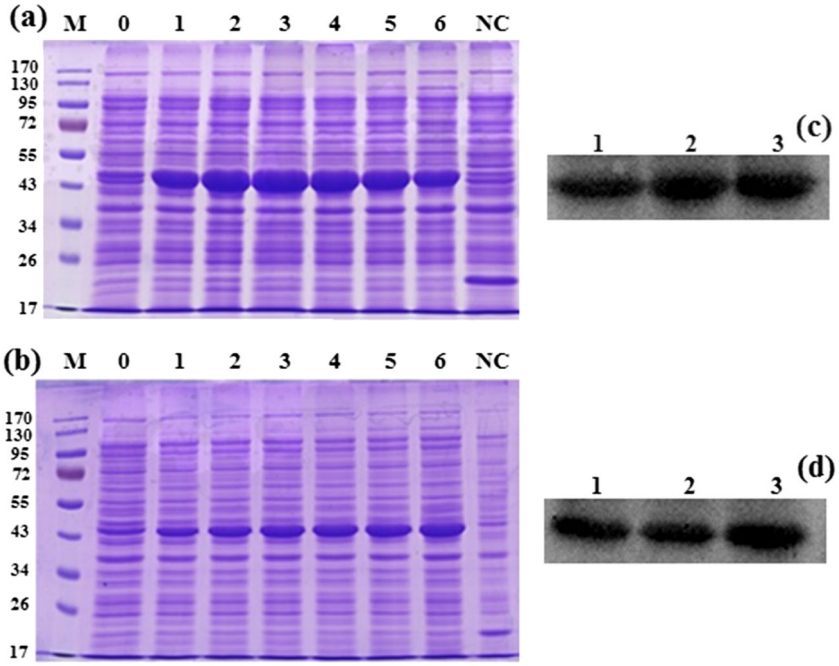

Fig. 7 SDS-PAGE electrophoresis and Western blot verification of phosphotriose isomerase protein expressed in a prokaryotic system. **a** *Demodex folliculorum* SDS-PAGE. **a** *Demodex brevis* SDS-PAGE. M: protein ladder (kDa); lane 0: 0 h; lane 1: 1 h; lane 2: 2 h; lane 3: 3 h; lane 4: 4 h; lane 5: 5 h; lane 6: 6 h. NC: pET32a, 4 h. **c** *Demodex folliculorum* Western blot. Lane 1: 1 h; lane 2: 2 h; lane 3: 3 h. **d** *Demodex brevis* Western blot. Lane 1: 2 h; lane 2: 3 h; lane 3: 6 h

Demodex species. A total of 10.2 and 10.8 ng of RNA were extracted from *D. folliculorum* and *D. brevis*, respectively. After RNA-Seq, 6.0996 ng and 6.9888 ng of RNA remained. Standard *TPI*, α-tubulin (*α-Tub*), and *Tm* plasmids had a high purity with OD_{260}/OD_{280} values that ranged from 1.94 to 2.02. The high amplification coefficients (0.9980–0.9997) and amplification efficiencies (88.39–99.53%) ensured that the established standard curves accurately reflected the gene amplification (Table 4). The results of absolute RT-qPCR showed the same expression trend for DEGs as those estimated by FPKM (Supplementary Fig. S4 and Table 3).

Discussion

Based on minimal available research on *Demodex* at the RNA level, this study was the first to complete de novo RNA-Seq and functional annotation of *D. folliculorum* and *D. brevis*. The four main breakthroughs of this study are as follows. First, with the aid of bioinformatics analysis combined with manual alignment, 237 CDSs were identified for 48 genes from 29 families of five important functional classes, namely "metabolic enzymes," "allergens," "motion-related," "detoxification and stress-response," and "mitochondrial." Second, through DEG analysis, expressional differences in important homologous functional genes were found to be implicated in pathogenicity differences between *D. folliculorum* and *D. brevis*. Third, by designing specific primers and constructing a prokaryotic expression system, PCR amplification, sequencing identification, and protein expression analysis were performed to adjust and verify the predicted CDSs. Fourth, based on the establishment of an absolute RT-qPCR method, DEG expression of *D. folliculorum* and *D. brevis* was verified.

This study provides preliminary insight into pathogenicity differences between *D. folliculorum* and *D. brevis*. In *D. folliculorum*, two important metabolism-related genes

Table 4 Absolute RT-qPCR results of the three DEGs between the two *Demodex* species

Gene	Species	SSC (ng/μL)	RE	CC	AE%	CTV	CN	Ratio*
TPI	*D. f*	37.52	$y = -3.2974x + 39.933$	0.9980	99.53	27.37	25,440	1.56
	D. b	49.48	$y = -3.4866x + 41.048$	0.9988	94.98	28.59	16,260	
α-Tub	*D. f*	74.87	$y = -3.5829x + 40.35$	0.9990	93.56	26.71	50,249	1.64
	D. b	63.33	$y = -3.6357x + 41.402$	0.9997	88.39	27.81	30,715	
Tm	*D. f*	99.98	$y = -3.516x + 40.829$	0.9995	92.80	25.91	178,294	1.72
	D. b	30.02	$y = -3.4771x + 41.417$	0.9996	93.90	25.54	103,421	

TPI triosephosphate isomerase, *α-Tub* α-tubulin, *Tm* tropomyosin, *D. f Demodex folliculorum*, *D. b Demodex brevis*, *SSC* standard sample concentration, *RE* regression equation, *CC* correlation coefficient, *AE* amplification efficiency, *CTV* cycle threshold value, *CN* copy number

**D.f* copy number vs *D.b* copy number

involved in the regulation of energy balance and glycolysis, namely arginine kinase and *TPI*, were highly expressed. This was in accordance with our previous in vitro observation that *D. folliculorum* is more active than *D. brevis* (Zhao et al. 2007). Motion-related genes such as muscle-specific protein 20-2, myosin basic light chain, tropomyosin, troponin C, and α-tubulin type 1 were also highly expressed in *D. folliculorum*, suggesting that mechanical lesions caused by the increased activity of *D. folliculorum* could be more serious than those caused by *D. brevis*. Dust mite allergens are the main components causing type I allergic diseases such as atopic dermatitis. This study screened and confirmed 10 allergen-encoding genes (Chan et al. 2015), of which *Der f* 1, *Der f* 27, *Der f* 20, *Der f* 25, *Der f* 29, *Der f* 26, *Der f* 10, *Der f* 33, and *Der f* 28 were highly expressed in *D. folliculorum*, indicating that this species might be implicated in erythema, papules, itching, and other symptoms of type I allergic reactions. In addition, the expression of detoxification and stress response genes in *D. folliculorum* was higher than that in *D. brevis*. This was probably because *D. folliculorum*, which inhabits shallow follicle funnels, would receive more external stimulation than *D. brevis*, which is found in deeper sebaceous glands. However, protein metabolism-associated enzymes such as aspartic protease, cathepsin, serine protease, chitinase, and chitin synthase were expressed at significantly higher levels in *D. brevis* than in *D. folliculorum*. This was especially true for aspartic protease, for which the FPKM value was 82.35 for *D. brevis* but which was not detected in *D. folliculorum*. As reported recently, aspartic protease can digest host skin and serum molecules, playing an important role in the ability of *Sarcoptes* to penetrate the keratin layer (Mahmood et al. 2013). We traced our previous transcriptome data for *Sarcoptes canis* (Hu et al. 2016) and found that the FPKM value of aspartic protease (819.87) was higher in *S. canis* than in *D. brevis*. Therefore, we speculate that aspartic protease facilitates *D. brevis* dermal penetration by inducing a type IV allergic reaction and causing the formation of skin nodules. We suggest that the differences in expression of important functional genes would be likely correlated with the pathogenic disparities between the two *Demodex* species. Therefore, we plan to elucidate the specific functions of these genes as related to the pathogenic differences between *D. folliculorum* and *D. brevis* in our future studies.

We also reported three technical achievements in this study. First, extracting high-quality RNA was a prerequisite for *Demodex* RNA-Seq. However, mites are among the smallest arthropods and have thick exoskeletons that are difficult to rupture. These two attributes make RNA-Seq difficult, which is reflected by the paucity of current information. In the SRA, limited transcriptome data can be retrieved for mites including *Sarcoptes*, *Dermanyssus*, *Dermatophagoides*, *Tyrophagus*, *Tetranychus*, *Panonychus*, *Neoseiulus*, and *Rhizoglyphus*. For *Demodex*, the smallest mites that have a body size of a few hundredths of that of *Psoroptes*, *Dermatophagoides*, or *Tetranychus*, RNA extraction was even more difficult (Zhao et al. 2016; Niu et al. 2017). In the beginning, the quantity and quality of extracted *Demodex* RNA were far from the requirements for RNA-Seq based on conventional RNA samples. Later, through repeated troubleshooting and improvement, we extracted RNA samples with RIN ≥ 5.0 and quantity ≥ 10 ng, which basically met the requirements for cDNA library construction of trace RNA proposed by the sequencing company (Hu et al. 2019). Thus, RNA-Seq was successfully completed for the two parasitic human *Demodex* species. It should be noted that the RNA quantity needed for RNA-Seq decreased from ≥ 200 (Hu et al. 2016) to ≥ 10 ng in the present study; specifically, the sequencing sensitivity increased 20-fold here. However, there were two notable limitations. One limitation was that Agilent 2100 detection showed a slightly elevated baseline, which indicated the slight degradation of RNA. The other was that the sample size was not big enough, as mites were obtained from relatively few sources and may represent only a genetic subsample of the entire population. The solution to both issues depends on the optimization of experimental conditions, including an increased sample size, and the improvement of RNA quality. These factors are important for subsequent *Demodex* RNA-Seq and functional gene research.

The second achievement was that CDS verification by specific primers was deemed essential for *Demodex* functional gene research. Although the advantages of de novo assembly include independence from reference sequences or alignment software, the disadvantage includes the merging of highly similar transcripts resulting in unavoidable errors. In our previous study on RNA-Seq for *S. canis*, some unigenes verified by specific primers were found to be incorrectly assembled (Hu et al. 2016). In this study, the verified CDSs of the two *Demodex* species were nearly consistent with the corresponding unigenes, except for *D. brevis Tm*, muscle protein alkaline light chain, and *TPI*, for which incorrect assembly or insertions and deletions of bases were detected in the unigenes. Overall, prokaryotic expression of the adjusted *TPI* sequence was successful. These findings suggest that it is inadvisable to directly use predicted CDSs for further functional research; instead, it is best to verify CDSs by PCR amplification and sequencing using specific primers.

The third achievement was the verification of expression by RT-qPCR, which is necessary to screen DEGs of the two *Demodex* species. FPKM is the most commonly used method to estimate gene expression levels, as it simultaneously considers the effect of sequencing depth and gene length for read counts. There are two types of RT-qPCR, namely relative and absolute quantification. Relative quantification can detect differences in expression of the same gene in the same species with different treatments or conditions, whereas absolute quantification can accurately quantify copy numbers of a gene in unknown samples, regardless of whether they are derived from the same

or different species (Sellars et al. 2007; Wang et al. 2013). In this study, *D. folliculorum* and *D. brevis* represent two different species of the genus *Demodex*, and thus, absolute and not relative quantification was more appropriate to verify differentially expressed homologous genes. Our results showed the same trend as the FPKM results, although differences were lower compared to those obtained by the latter method. This is because Illumina transcriptome sequencing, presently the most popular next-generation sequencing platform, has a higher sensitivity than RT-qPCR as it can detect rare transcripts. However, RT-qPCR is universally recognized as a stable and specific early detection method to assess expression quantities. Therefore, performing RT-qPCR verification of results obtained by RNA-Seq is recommended. This ensures not only robustness, but also reliability, with increased sample sizes.

In summary, we performed the first successful RNA-Seq and functional annotation analysis of *Demodex*. This not only could form the basis for research on differential functional genes and pathogenicity in *Demodex* species but also provides a reference for the collection of sufficient genetic data from other organisms with similar limitations (small body size, hard chitinous exoskeleton, or limited sources), as well as rare and precious samples. With the continuous improvement of molecular biological technologies, genome-wide sequencing and research on important *Demodex* functional genes is possible. These findings will enable breakthroughs in revealing the pathogenesis of demodicidosis, in addition to eventually mitigating the threat of *Demodex* species to humans.

Funding information This work was supported by National Natural Science Foundation of China (Nos. 81471972 and 81271856).

Compliance with ethical standards The present study was approved by the Ethics Committee of Medical and Biological Research of Xi'an Jiaotong University Health Science Center (approval no. 2019-002). All subjects were sampled by the authors or associated project staff. Written informed consent was obtained from all patients.

Conflict of interest On behalf of all authors, the corresponding author states that there is no conflict of interest.

References

Ayres SJ (1930) Pityriasis folliculorum (*Demodex*). Arch Dermatol Syphilol 21:19–24. https://doi.org/10.1001/archderm.1930.01440070027002

Chan TF, Ji KM, Yim AK, Liu XY, Zhou JW, Li RQ, Yang KY, Li J, Li M, Law PT, Wu YL, Cai ZL, Qin H, Bao Y, Leung RK, Ng PK, Zou J, Zhong XJ, Ran PX, Zhong NS, Liu ZG, Tsui SK (2015) The draft genome, transcriptome, and microbiome of *Dermatophagoides farinae* reveal a broad spectrum of dust mite allergens. J Allergy Clin Immunol 135:539–548. https://doi.org/10.1016/j.jaci.2014.09.031

Cheng S, Zhang M, Chen H, Fan W, Huang Y (2019) The correlation between the microstructure of meibomian glands and ocular *Demodex* infestation: a retrospective case-control study in a Chinese population. Medicine (Baltimore) 98:e15595. https://doi.org/10.1097/MD.0000000000015595

Conte YL, Alaux C, Martin JF, Harbo JR, Harris JW, Dantec C, Navajas M (2011) Social immunity in honeybees (Apis mellifera): transcriptome analysis of varroa-hygienic behaviour. Insect Mol Biol 20:399–408. https://doi.org/10.1111/j.1365-2583.2011.01074.x

Cornall K, Wall R (2015) Ectoparasites of goats in the UK. Vet Parasitol 207:176–179. https://doi.org/10.1016/j.vetpar.2014.11.005

Ferrer L, Ravera I, Silbermayr K (2014) Immunology and pathogenesis of canine demodicosis. Vet Dermatol 25:427–e65. https://doi.org/10.1111/vde.12136

Forton F (2012) Papulopustular rosacea, skin immunity and *Demodex*: pityriasis folliculorum as a missing link. J Eur Acad Dermatol Venereol 26:19–28. https://doi.org/10.1111/j.1468-3083.2011.04310.x

Gazi U, Gureser AS, Oztekin A, Karasartova D, Kosar-Acar N, Derici MK, Artuz F, Mumcuoglu KY, Taylan-Ozkan A (2019) Skin-homing T-cell responses associated with *Demodex* infestation and rosacea. Parasite Immunol 24:e12658. https://doi.org/10.1111/pim.12658

Grbić M, Van Leeuwen T, Clark RM, Rombauts S, Rouzé P, Grbić V, Osborne EJ, Dermauw W, Ngoc PC, Ortego F, Hernández-Crespo P, Diaz I, Martinez M, Navajas M, Sucena É, Magalhães S, Nagy L, Pace RM, Djuranović S, Smagghe G, Iga M, Christiaens O, Veenstra JA, Ewer J, Villalobos RM, Hutter JL, Hudson SD, Velez M, Yi SV, Zeng J, Pires-daSilva A, Roch F, Cazaux M, Navarro M, Zhurov V, Acevedo G, Bjelica A, Fawcett JA, Bonnet E, Martens C, Baele G, Wissler L, Sanchez-Rodriguez A, Tirry L, Blais C, Demeestere K, Henz SR, Gregory TR, Mathieu J, Verdon L, Farinelli L, Schmutz J, Lindquist E, Feyereisen R, Van de Peer Y (2011) The genome of *Tetranychus urticae* reveals herbivorous pest adaptations. Nature 2479:487–492. https://doi.org/10.1038/nature10640

He ML, Xu J, He R, Shen NX, Gu XB, Peng XR, Yang GY (2016) Preliminary analysis of *Psoroptes ovis* transcriptome in different developmental stages. Parasite Vector 9(570):570. https://doi.org/10.1186/s13071-016-1856-z

Hoy MA, Yu FH, Meyer JM, Tarazona OA, Jeyaprakash A, Wu K (2013) Transcriptome sequencing and annotation of the predatory mite *Metaseiulus occidentalis* (Acari: Phytoseiidae): a cautionary tale about possible contamination by prey sequences. Exp Appl Acarol 59:283–296. https://doi.org/10.1007/s10493-012-9603-4

Hu L, Zhao YE, Cheng J, Yang Y, Li C, Lu ZH (2015) Constructing and detecting a cDNA library for mites. Parasitol Res 114:3893–3901. https://doi.org/10.1007/s00436-015-4621-x

Hu L, Zhao YE, Yang YJ, Niu DL, Wang RL, Cheng J, Yang F (2016) *De novo* RNA-Seq and functional annotation of *Sarcoptes scabiei canis*. Parasitol Res 115:2661–2670. https://doi.org/10.1007/s00436-016-5013-6

Hu L, Zhao YE, Niu DL, Yang R (2019) Establishing an RNA extraction method from a small number of *Demodex* mites for transcriptome sequencing. Exp Parasitol 200:67–72. https://doi.org/10.1007/s00436-015-4815-2

Kabululu ML, Ngowi HA, Kimera SI, Lekule FP, Kimbi EC, Johansen MV (2015) Risk factors for prevalence of pig parasitoses in Mbeya Region, Tanzania. Vet Parasitol 212:460–464. https://doi.org/10.1016/j.vetpar.2015.08.006

Liu B, Jiang GF, Zhang YF, Li JL, Li XJ, Yue JS, Chen F, Liu H, Li H, Zhu S, Wang J, Ran C (2011) Analysis of transcriptome differences between resistant and susceptible strains of the citrus red mite *Panonychus citri* (Acari: Tetranychidae). PLoS One 6:e28516. https://doi.org/10.1371/journal.pone.0028516

Mahmood W, Viberg LT, Fischer K, Walton SF, Holt DC (2013) An aspartic protease of the scabies mite *Sarcoptes scabiei* is involved in the digestion of host skin and blood macromolecules. Plos Neglect Trop D 7(2525):e2525. https://doi.org/10.1371/journal.pntd.0002525

Niu DL, Wang RL, Zhao YE, Yang R, Hu L, Lei YY, Dan WC (2017) cDNA library construction of two human *Demodex* species. Acta Parasitol 62:354–376. https://doi.org/10.1515/ap-2017-0043

Olinda RG, Frade MTS, Soares GSL, de Aguiar GMN, Costa VMD, de Lucena RB, Dantes AFM (2013) Bovine demodicosis associated with squamous cell carcinoma of the vulva. Acta Sci Vet 41:29

Schicht S, Qi WH, Poveda L, Strube C (2013) The predicted secretome and transmembranome of the poultry red mite *Dermanyssus gallinae*. Parasite Vector 6:259. https://doi.org/10.1186/1756-3305-6-259

Sellars MJ, Vuocolo T, Leeton LA, Coman GJ, Degnan BM, Preston NP (2007) Real-time RT-PCR quantification of Kuruma shrimp transcripts: a comparison of relative and absolute quantification procedures. J Biotechnol 129:391–399. https://doi.org/10.1016/j.jbiotec.2007.01.029

Stuglik MT, Babik W, Prokop Z, Radwan J (2014) Alternative reproductive tactics and sex-biased gene expression: the study of the bulb mite transcriptome. Ecol Evol 4:623–632. https://doi.org/10.1002/ece3.965

Wang DT, Guo QQ, Zhu HW, Liu Z, Wang GW, Li CY (2013) Comparative studies between relative and absolute PCR value using Sika Deer P21 gene as an example. Spec Wild Econ Anim Plant Res 4:10–13. https://doi.org/10.16720/j.cnki.tcyj.2013.04.014

Zeytun E, Yazici M (2019) Incidence and density of *Demodex folliculorum* and *Demodex brevis* (Acari: Demodicidae) in patients with acne in the province of Erzincan, Turkey. Int J Acarol 45:108–112. https://doi.org/10.1080/01647954.2018.1564790

Zhao YE (2016) Human demodicosis: emerging dermatosis caused by *Demodex*. Chin J Parasitol Parasit Dis 34:456–462,472

Zhao YE, Guo N, Li C, Lu ZH (2007) The dynamic observation of the morphologic structure and activity of human *Demodex* in different stages. Chin J Vector Bio Control 18:120–123. https://doi.org/10.3969/j.issn.1003-4692.2007.02.013

Zhao YE, Guo N, Wu LP (2009) The effect of temperature on the viability of *Demodex folliculorum* and *Demodex brevis*. Parasitol Res 105:1623–1628. https://doi.org/10.1007/s00436-009-1603-x

Zhao YE, Wu LP, Peng Y, Cheng H (2010) Retrospective analysis of the association between *Demodex* infestation and rosacea. Arch Dermatol 146:896–902. https://doi.org/10.1001/archdermatol.2010.196

Zhao YE, Guo N, Xun M, Xu JR, Wang M, Wang DL (2011a) Sociodemographic characteristics and risk factor analysis of *Demodex* infestation (Acari: Demodicidae). J Zhejiang Univ-Sci B 12:998–1007. https://doi.org/10.1631/jzus.B1100079

Zhao YE, Peng Y, Wang XL, Wu LP, Wang M, Yan HL, Xiao SX (2011b) Facial dermatosis associated with *Demodex*: a case–control study. J Zhejiang Univ-Sci B 12:1008–1015. https://doi.org/10.1631/jzus.B1100179

Zhao YE, Guo N, Wu LP (2011c) Influence of temperature and medium on viability of *Demodex folliculorum* and *Demodex brevis* (Acari: Demodicidae). Exp Appl Acarol 54:421–425. https://doi.org/10.1007/s10493-011-9445-5

Zhao YE, Wu LP, Hu L, Xu JR (2012a) Association of blepharitis with *Demodex*: a meta-analysis. Ophthal Epidemiol 19:95–102. https://doi.org/10.3109/09286586.2011.642052

Zhao YE, Hu L, Wu LP, Ma JX (2012b) A meta-analysis of association between acne vulgaris and *Demodex* infestation. J Zhejiang Univ-Sci B 13:192–202. https://doi.org/10.1631/jzus.B1100285

Zhao YE, Hu L, Ma JX (2013) Molecular identification of four phenotypes of human *Demodex* mites (Acari: Demodicidae) based on mitochondrial 16S rDNA. Parasitol Res 112:3703–3711. https://doi.org/10.1007/s00436-013-3558-1

Zhao YE, Hu L, Yang YJ, Niu DL, Wang RL, Li WH, Ma SJ, Cheng J (2016) Improvement on the extraction method of RNA in mites and its quality test. Parasitol Res 115:851–858. https://doi.org/10.1007/s00436-015-4815-2